A Novel Fast Transient Current Scheme for Three Phase Dual Active Bridge with Asymmetrical Phase-Shift Control

Hui Chen, Jinjun Liu, Sixing Du, Cong Li, and Zhifeng Deng
State Key Lab of Electrical Insulation and Power Equipment
School of Electrical Engineering, Xi'an Jiaotong University
Xi'an China

***Abstract*-- It is well-known issue that dc bias and oscillations will be introduced into phase current and dc current when the transmission power and control variables of three phase dual active bridge (3ph-DAB) converter have the abrupt changes. It will cause the magnetic saturation problem and degrade the dynamic response seriously. To solve this issue, this paper proposes a novel fast transient current control scheme with asymmetrical three phase (APS) control. By choosing suitable transient phase shift angles, the proposed method can greatly suppress the dc bias and overshoot of phase current and improve the transient performance significantly. It is presented to make 3ph-DAB transit from initial steady state to target steady state within one step through the proposed method and space-vector theory. The simulation results verify the effectiveness of proposed scheme.**

***Index Terms*--3ph-DAB, improve dynamic response, APS control, fast transient Current control.**

I. INTRODUCTION

To deal with the growing serious energy crisis, development of renewable energy technology such as photovoltaic power generation, energy storage system and dc distribution grid has become one of the major approaches to solve the challenge of energy shortage[1], [2]. The isolated bidirectional DC/DC converter (IBDC) as the popular converter is widely used in above renewable energy applications. And the 3ph-DAB has been well recognized as one of promising topologies for IBDC due to its many obvious advantages. Compared with other investigated IBDC topologies, 3ph-DAB is the preferred choice to be applied in the high-power industry application because of its superiority to transfer higher power with lower RMS current, smaller component stress, higher power density, inherent soft-switching operation, bidirectional power transmission and buck-boost capability[3]–[7].

The transient performance of 3ph-DAB is a critical issue in the practical work. When the transferred power has an abrupt change, the control variables of 3ph-DAB will be step changed. It will bring the dc bias and overshoot of phase current and it will bring the serious magnetic saturation problem of the transformer. According to [8]–[10], the dc bias of phase current and oscillations will decay with the time constant $\tau = L\sigma/R$. Where $L\sigma$ and R are the leakage inductance and resistance of the transformer. Because of achieving high efficiency, winding resistance is very low and the oscillations will last long and it degrades the dynamic performance of 3ph-DAB significantly. To cope with this problem, two instantaneous current control (ICC) methods have been proposed in [8]–[10]. These ICC methods adopt intermediate phase shift angles to make 3ph-DAB converter reach new steady state within two or three steps. However, these methods have been only used in conventional single phase-shift (SPS) modulation. The fast transient current control (FTCC) method is proposed in [11], [12] to improve the transient performance by means of variable duty cycle control. This scheme enables 3ph-DAB to reach new steady state within two steps. All these control methods are based on the symmetrical three phase control of 3ph-DAB. In fact, the asymmetrical three phase control of 3ph-DAB called as APS control will provide more freedoms to improve performance and it was proposed in [13]. The dynamic optimization based on APS control has not been investigated. This paper proposes a novel fast transient current control of 3ph-DAB with APS control. Adopting the proposed method, the dynamic performance is improved and 3ph-DAB converter can reach new steady state within one step.

II. FUNDAMENTAL ANALYSIS OF APS CONTROL

The 3ph -DAB topology is shown in the Fig. 1. This topology comprises two three-phase active bridges at both sides connected by three phase inductors and high frequency transformers with turn ratio N_{12}. V_{1x} (x=a,b,c) and V_{2x} are the phase voltage in the both sides. i_{La}, i_{Lb}, and i_{Lc} are the phase currents. $S_{xy}(t)$ (x = 1 and 2; y = a, b, and c) are the switching functions of primary and secondary sides. The value of $S_{xy}(t)$ is equal to 1, which implies that the upper switch of the corresponding side and phase is on and the lower switch is off. The reverse is also true. According to the switching function, the phase voltage V_{1x} and V_{2x} can be derived as formula (1).

$$\begin{cases} v_{1a}(t) = \dfrac{V_1(2S_{1a}(t) - S_{1b}(t) - S_{1c}(t))}{3} \\ v_{1b}(t) = \dfrac{V_1(2S_{1b}(t) - S_{1a}(t) - S_{1c}(t))}{3} \\ v_{1c}(t) = \dfrac{V_1(2S_{1c}(t) - S_{1b}(t) - S_{1a}(t))}{3} \\ v_{2a}(t) = \dfrac{N_{12}V_2(2S_{2a}(t) - S_{2b}(t) - S_{2c}(t))}{3} \\ v_{2b}(t) = \dfrac{N_{12}V_2(2S_{2b}(t) - S_{2a}(t) - S_{2c}(t))}{3} \\ v_{2c}(t) = \dfrac{N_{12}V_2(2S_{2c}(t) - S_{2b}(t) - S_{2a}(t))}{3} \end{cases} \quad (1)$$

In the APS control, the variable phase-shift angles instead of fixed 1/3 among the three-phase legs are employed. All phase legs have same duty cycle which is equal to 0.5 and the phase shift angles among phase legs and both active bridges keep adjustable. As the Fig. 2 shown, for analysis simplification, assume that inner phase shift angles of both bridges are the same. Hence, there are three control variables including D_1, D_2 which denote the variable phase-shift angles between phases B & A and C & A in both sides and D_3 which denotes phase-shift angle between primary and secondary bridges to control the power transferred.

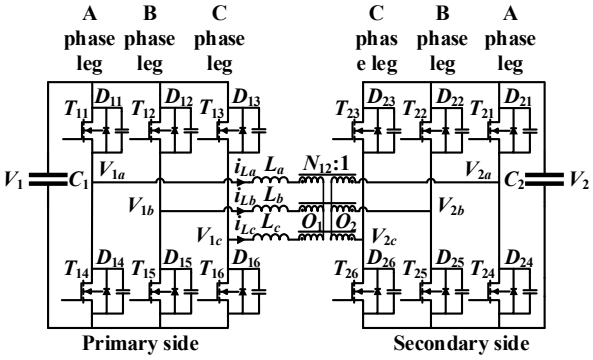

Fig. 1. Circuit schematic of 3ph-DAB.

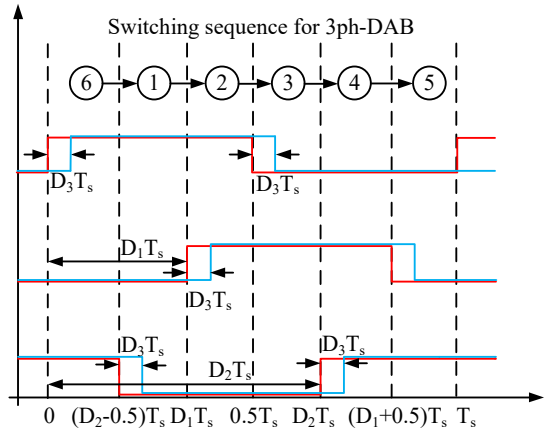

Fig. 2. Switching sequence of 3ph-DAB with APS control.

In the APS control, the adjustable phase-shift angles D_1, D_2, D_3 will generate asymmetrical five-level AC sources on both sides. However, the voltage seconds over the entire switching period are always balanced. This ensures that the phase currents have no dc bias and the magnetic saturation problem will be avoided in the steady state. According to the formula (1), the conclusion can be deduced.

$$v_{1a}(t)+v_{1b}(t)+v_{1c}(t)=0, v_{2a}(t)+v_{2b}(t)+v_{2c}(t)=0$$
$$i_{La}(t)+i_{La}(t)+i_{Lb}(t)=0 \quad (2)$$

Formula (2) implies that phase voltage and current have no zero sequence components. It means that phase voltage and current can be synthesized as the space vectors in αβ coordinates. In the APS modulation, 3ph-DAB operates as six switching states in each switching period. It is presented in the Table I. The primary and secondary voltage vector can be expressed associated with switching states, $\overrightarrow{u_p}=\frac{2}{3}V_1\cdot\overrightarrow{b_n}(n=1,2...6)$, $\overrightarrow{u_s}=\frac{2}{3}d\cdot V_1\cdot\overrightarrow{b_n}$,where d=$N_{12}V_2/V_1$. And the equivalent circuit can be built up as Fig. 3 shown. In the equivalent circuit, the magnetizing inductor is enough large to be neglected. Refer to the Fig. 3, phase current vector can be presented as: $\frac{d\vec{i_p}}{dt}=\frac{\overrightarrow{u_p}-\overrightarrow{u_s}}{L_s}$. Based on above formula and switching sequence for 3ph-DAB shown in Fig. 2, the variation of phase current vector from switching sate m to m+1 can be derived. For example, the variation of phase current vector from switching sate 5 to 6 can be deduced as follows

Large figures and tables may span both columns but may not extend into the page margins. Figure captions must be below the figures; table captions have to be above the tables.

$$\Delta\vec{i}_{p,5\to6}(D_3T_s)=D_3T_s\cdot(\frac{2}{3}V_1\cdot\overrightarrow{b_6}-\frac{2}{3}dV_1\cdot\overrightarrow{b_5})$$
$$+(D_2-0.5-D_3)T_s\cdot(\frac{2}{3}V_1\cdot\overrightarrow{b_6}-\frac{2}{3}dV_1\cdot\overrightarrow{b_6}) \quad (3)$$

Other variation of phase current vector between two successive switching states can be derived similarly. Then the trajectory of phase current can be drawn in αβ coordinates like the Fig. 4 shown (φ=D_3*T_s).

TABLE I
SWITCHING STATE OF 3PH-DAB

Switching state	1	2	3	4	5	6
$S_{1a}(t)$, $S_{2a}(t)$	1	1	0	0	0	1
$S_{1b}(t)$, $S_{2b}(t)$	0	1	1	1	0	0
$S_{1c}(t)$, $S_{2c}(t)$	0	0	0	1	1	1
Switching vector	$\overrightarrow{b_1}$	$\overrightarrow{b_2}$	$\overrightarrow{b_3}$	$\overrightarrow{b_4}$	$\overrightarrow{b_5}$	$\overrightarrow{b_6}$

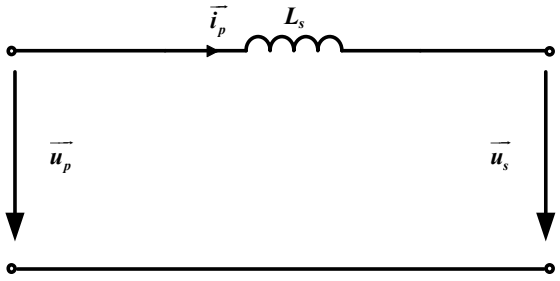

Fig. 3. The equivalent circuit of 3ph-DAB.

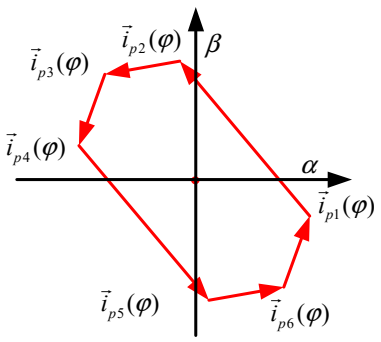

Fig. 4. The phase current trajectory of 3ph-DAB with APS control

III. Fast Transient Current Scheme With APS Control

A. Conventional scheme

For the conventional transient modulation in 3ph-DAB, the inner and outer phase shift angles will have the abrupt changes simultaneously when the 3ph-DAB converter operates from initial steady state (D_{11}, D_{21}, D_{31}) to new target state (D_{12}, D_{22}, D_{32}). As the Fig. 5 shown, the center of the transient current trajectory is shift from origin because of these abrupt changes of control variables and it cannot track up target current trajectory effectively[10]. It means that the dc bias and oscillations will occur in three phase currents. According to the [8], [9], the oscillations decay time is very large and oscillations will last long. It will degrade the dynamic performance of 3ph-DAB significantly.

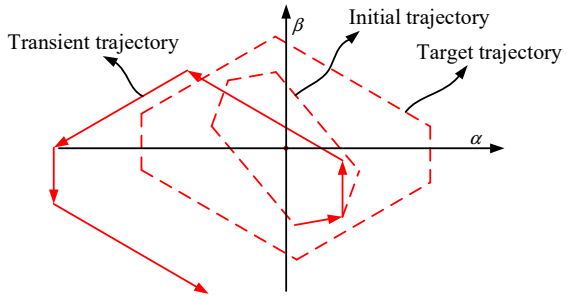

Fig. 5. Conventional transient modulation in 3ph-DAB with APS control

B. A novel fast transient current scheme with APS control

If the center of the transient current trajectory can be shift back to the origin in αβ coordinates within short time, the dynamic performance of 3ph-DAB will be greatly improved. This part will propose a novel fast transient current scheme with APS control and this control method can track up the target current trajectory within one step.

The novel fast transient current scheme can be demonstrated in the Fig. 6. In the Fig. 6, ϕ_1=D_{31}*T_s and ϕ_2=D_{32}*T_s. Assume that 3ph-DAB operates under initial and target steady states with D_{11}, D_{21} D_{31} and D_{12}, D_{22} D_{32} respectively. Then, according to the switching sequence of 3ph-DAB with APS control in Fig. 2, Fig. 7 and the formula (3) of phase current variation, these key current vectors can be derived.

$$\vec{i}_{p6}(\varphi_1)=\frac{((-1+d)(2+D_{11}-3D_{21})+2d\cdot D_{31})\frac{2}{3}V_1\cdot T_s}{4L_s}$$
$$+i\cdot\frac{-\sqrt{3}((-1+d)(D_{11}-D_{21})+2d\cdot D_{31})\frac{2}{3}V_1\cdot T_s}{4L_s} \quad (4)$$
$$\vec{i}_{p1}(\varphi_2)=\frac{(-3(-1+d)D_{12}+(-1+d)D_{22}+4d\cdot D_{32})\frac{2}{3}V_1\cdot T_s}{4L_s}$$
$$+i\cdot\frac{-\sqrt{3}(-1+d)(D_{12}-D_{22})\frac{2}{3}V_1\cdot T_s}{4L_s}$$

The blue vector is the transient current trajectory by adopting proposed fast transient current control scheme. As the Fig. 6 and 7 shown, by means of the blue vector (transient current vector), 3ph-DAB can transit from initial steady state to target steady state within one step. In this transition process shown in Fig. 6 and 7, the transient outer phase shift angle is defined as D_{33} and the transient current vector can be derived based on formula (3), (4):

$$\Delta\vec{i}_{p,6\to1}(\varphi_1\to\varphi_2)=D_{33}T_s\cdot\frac{\frac{2}{3}d\cdot V_1}{L_s}(\vec{b}_1-\vec{b}_6)$$
$$+(D_{12}+0.5-D_{21})T_s\cdot(\frac{\frac{2}{3}\cdot V_1}{L_s}-\frac{\frac{2}{3}d\cdot V_1}{L_s})(\vec{b}_1)=\vec{i}_{p1}(\varphi_2)-\vec{i}_{p6}(\varphi_1) \quad (5)$$

By solving the formula (5), the transient outer phase shift angle D_{33} can be derived:

$$D_{33}=\frac{(-1+d)(D_{11}-D_{12}-D_{21}+D_{22})}{2d}+D_{31} \quad (6)$$

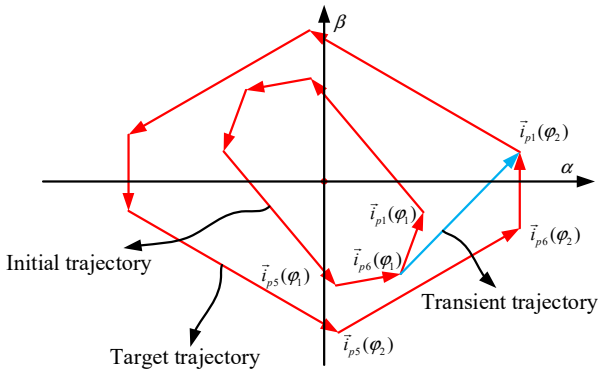

Fig. 6. Trajectory of transition process with proposed method

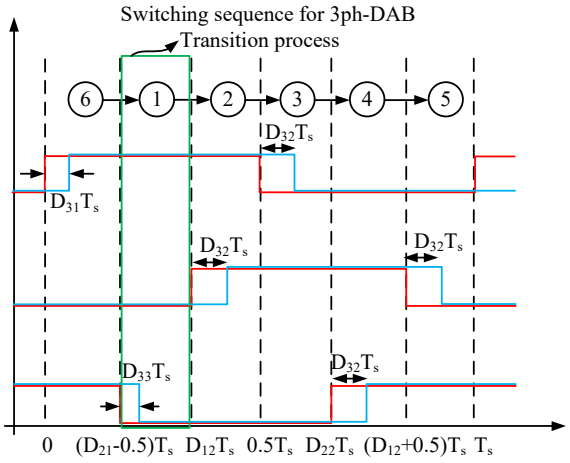

Fig. 7. Switching sequence of proposed method

As long as the value of D_{33} is chosen based on formula (6), the 3ph-DAB can reach the new target steady state quickly within one step.

IV. Simulation Results

To verify the effectiveness of proposed fast transient current scheme with APS control, the simulation models of proposed and conventional methods are built up in

PLECS. Both of methods have the same parameters of main circuit, phase shift angles of steady state and the transferred power changed from 3978.87W to 12784.4W at the t=0.2s which are listed in Table II. The switching frequency of 3ph-DAB is 10kHz.

TABLE II
PARAMETERS OF SIMULATION RESULTS

Modulation method	In/out voltage	Lσ/R	power	Phase shift angles
Conventional method	1000V/ 600V	0.2mH /0.01 Ω	3978.87W (0<t<0.2)	D_1=0.25, D_2=0.6, D_3=0.02 (initial steady state at 10kHz) D_1=0.4, D_2=0.7, D_3=0.07 (transient state at 10kHz) D_1=0.4, D_2=0.7, D_3=0.07 (target steady state at 10kHz)
Proposed method	1000V/ 600V	0.2mH /0.01 Ω	12784.4W (t>0.2)	D_1=0.25, D_2=0.6, D_3=0.02 (initial steady state at 10kHz) D_1=0.25, D_2=0.7 D_3=0.037 (transient state at 10kHz) D_1=0.4, D_2=0.7, D_3=0.07 (target steady state at 10kHz)

Fig. 8 and 9 illustrates the comparison of dynamic response in proposed scheme and conventional method. Fig. 8 shows the transient response of phase current by adopting conventional method. The dc bias will introduce into the phase current and the dynamic behavior of phase current will last over 48.979 ms. Fig. 9 shows the transient response of phase current by using proposed scheme with APS control. it is obvious that the dynamic response of phase current has been improved significantly and the transient interval is shortened to 40 us. Hence, this comparison reveals conclusions that adopting proposed scheme can obtain the extremely better dynamic performance than using conventional method.

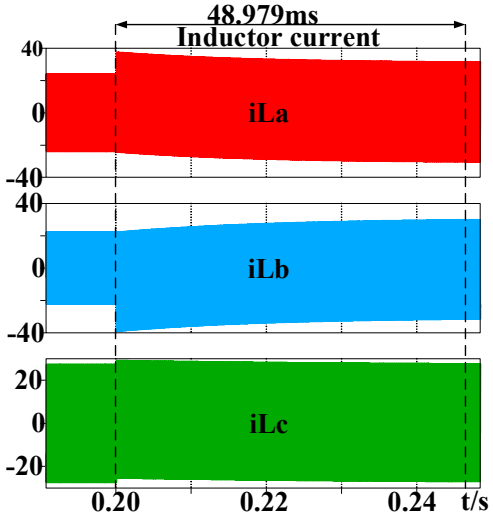

Fig. 8. Dynamic response of conventional method

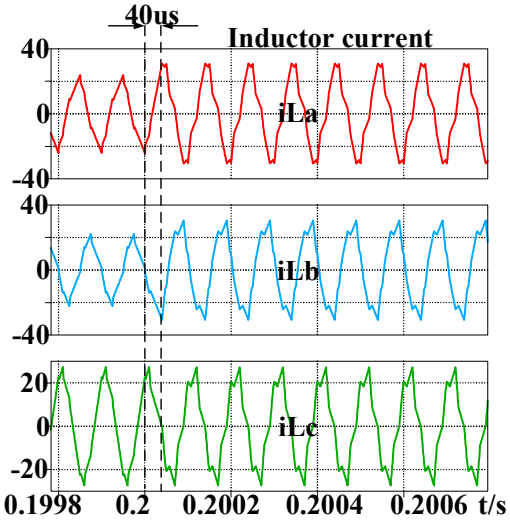

Fig. 9. Dynamic response of proposed method

V. CONCLUSIONS

This paper proposes a novel fast transient current scheme with APS control to improve the dynamic response of 3ph-DAB. This proposed method can make 3ph-DAB reach new steady state within one step. The transient phase shift angles can be deduced by using the space vector method. Compared with conventional method, the proposed method realizes the extremely better transient performance and simulation results verify the effectiveness of theory.

REFERENCES

[1] B. Zhao, Q. Song, W. Liu, and Y. Sun, "Overview of Dual-Active-Bridge Isolated Bidirectional DC–DC Converter for High-Frequency-Link Power-Conversion System," *IEEE Trans. Power Electron.*, vol. 29, no. 8, pp. 4091–4106, Aug. 2014.

[2] N. Hou and Y. W. Li, "Overview and Comparison of Modulation and Control Strategies for a Nonresonant Single-Phase Dual-Active-Bridge DC–DC Converter," *IEEE Trans. Power Electron.*, vol. 35, no. 3, pp. 3148–3172, Mar. 2020.

[3] Z. Li, Y. Wang, L. Shi, J. Huang, Y. Cui, and W. Lei, "Generalized averaging modeling and control strategy for three-phase dual-active-bridge DC-DC converters with three control variables," *in 2017 IEEE Applied Power Electronics Conference and Exposition (APEC)*, Tampa, FL, USA, Mar. 2017, pp. 1078–1084.

[4] S. P. Engel, M. Stieneker, N. Soltau, S. Rabiee, H. Stagge, and R. W. De Doncker, "Comparison of the Modular Multilevel DC Converter and the Dual-Active Bridge Converter for Power Conversion in HVDC and MVDC Grids," *IEEE Trans. Power Electron.*, vol. 30, no. 1, pp. 124–137, Jan. 2015.

[5] R. W. A. A. De Doncker, D. M. Divan, and M. H. Kheraluwala, "A three-phase soft-switched high-power-density DC/DC converter for high-power applications," *IEEE Trans. Ind. Appl.*, vol. 27, no. 1, pp. 63–73, Jan. 1991.

[6] J. Huang, Y. Wang, Z. Li, and W. Lei, "Multifrequency approximation and average modelling of an isolated

bidirectional dc–dc converter for dc microgrids," *IET Power Electron*., vol. 9, no. 6, pp. 1120–1131, 2016.
[7] L. M. Cúnico, Z. M. Alves, and A. L. Kirsten, "Efficiency-Optimized Modulation Scheme for Three-Phase Dual-Active-Bridge DC–DC Converter," *IEEE Trans. Ind. Electron*., vol. 68, no. 7, pp. 5955–5965, Jul. 2021.
[8] S. P. Engel, N. Soltau, H. Stagge, and R. W. De Doncker, "Dynamic and Balanced Control of Three-Phase High-Power Dual-Active Bridge DC–DC Converters in DC-Grid Applications," *IEEE Trans. Power Electron*., vol. 28, no. 4, pp. 1880–1889, Apr. 2013.
[9] S. P. Engel, N. Soltau, H. Stagge, and R. W. De Doncker, "Improved Instantaneous Current Control for High-Power Three-Phase Dual-Active Bridge DC–DC Converters," *IEEE Trans. Power Electron*., vol. 29, no. 8, pp. 4067–4077, Aug. 2014.
[10] J. Hu, S. Cui, S. Wang, and R. W. De Doncker, "Instantaneous Flux and Current Control for a Three-Phase Dual-Active Bridge DC–DC Converter," *IEEE Trans. Power Electron*., vol. 35, no. 2, pp. 2184–2195, Feb. 2020.
[11] Z. Li, Y. Wang, Y. Cui, L. Shi, J. Huang, and W. Lei, "Fast transient current control for three-phase dual-active-bridge dc-dc converters with variable duty cycles," *in 2017 IEEE Applied Power Electronics Conference and Exposition (APEC)*, Mar. 2017, pp. 1209–1215.
[12] J. Huang, Z. Li, L. Shi, Y. Wang, and J. Zhu, "Optimized Modulation and Dynamic Control of a Three-Phase Dual Active Bridge Converter With Variable Duty Cycles," *IEEE Trans. Power Electron*., vol. 34, no. 3, pp. 2856–2873, Mar. 2019.
[13] H. Chen, S. Ouyang, J. Liu, and X. Li, "An Asymmetrical Phase-Shift Scheme of Three-Phase Dual Active Bridge With Minimum Current Root-Mean-Square Value Control," *IEEE Trans. Power Electron*., vol. 37, no. 12, pp. 14343–14361, Dec. 2022.